

RankSteer: Activation Steering for Pointwise LLM Ranking

Yumeng Wang

y.wang@liacs.leidenuniv.nl

Leiden Institute of Advanced
Computer Science, Leiden University
Leiden, The Netherlands

Catherine Chen

catherine_s_chen@brown.edu

Brown University
Providence, RI, USA

Suzan Verberne

s.verberne@liacs.leidenuniv.nl

Leiden Institute of Advanced
Computer Science, Leiden University
Leiden, The Netherlands

Abstract

Large language models (LLMs) have recently shown strong performance as zero-shot rankers, yet their effectiveness is highly sensitive to prompt formulation, particularly role-play instructions. Prior analyses suggest that role-related signals are encoded along activation channels that are largely separate from query-document representations, raising the possibility of steering ranking behavior directly at the activation level rather than through brittle prompt engineering. In this work, we propose RankSteer, a post-hoc activation steering framework for zero-shot pointwise LLM ranking. We characterize ranking behavior through three disentangled and steerable directions in representation space: a **decision direction** that maps hidden states to relevance scores, an **evidence direction** that captures relevance signals not directly exploited by the decision head, and a **role direction** that modulates model behavior without injecting relevance information. Using projection-based interventions at inference time, RankSteer jointly controls these directions to calibrate ranking behavior without modifying model weights or introducing explicit cross-document comparisons. Experiments on TREC DL 20 and multiple BEIR benchmarks show that RankSteer consistently improves ranking quality using only a small number of anchor queries, demonstrating that substantial ranking capacity remains under-utilized in pointwise LLM rankers. We further provide a geometric analysis revealing that steering improves ranking by stabilizing ranking geometry and reducing dispersion, offering new insight into how LLMs internally represent and calibrate relevance judgments.

CCS Concepts

- Information systems → Information retrieval; Retrieval models and ranking.

Keywords

Pointwise Ranking, Interpretability, Activation steering, Role-play, Large Language Models

ACM Reference Format:

Yumeng Wang, Catherine Chen, and Suzan Verberne. 2018. RankSteer: Activation Steering for Pointwise LLM Ranking. In *Proceedings of Make sure to enter the correct conference title from your rights confirmation email*

Permission to make digital or hard copies of all or part of this work for personal or classroom use is granted without fee provided that copies are not made or distributed for profit or commercial advantage and that copies bear this notice and the full citation on the first page. Copyrights for components of this work owned by others than the author(s) must be honored. Abstracting with credit is permitted. To copy otherwise, or republish, to post on servers or to redistribute to lists, requires prior specific permission and/or a fee. Request permissions from permissions@acm.org.

Conference acronym 'XX, Woodstock, NY

© 2018 Copyright held by the owner/author(s). Publication rights licensed to ACM.

ACM ISBN 978-1-4503-XXXX-X/2018/06

<https://doi.org/XXXXXX.XXXXXXX>

(Conference acronym 'XX). ACM, New York, NY, USA, 11 pages. <https://doi.org/XXXXXX.XXXXXXX>

1 Introduction

Recent work has shown that large language models (LLMs) can serve as powerful zero-shot rankers, but their performance depends critically on prompt formulation [30]. In particular, assigning a functional role to the model – a practice known as role-play prompting – can dramatically alter the quality of the rankings. As illustrated in Figure 1(a,b), framing the same pointwise ranking prompt with different roles (e.g., “reliable” versus “careless” search assistant) leads to large shifts in retrieval metrics [37]. These observations indicate that even minor changes in role phrasings can strongly influence how LLMs judge relevance. Mechanistic analyses deepen this picture. For instance, causal intervention (“patching” [20, 39]) experiments reveal that role-play instructions and the query-document context are processed largely independently in the model’s hidden layers. Role-related signals tend to be encoded in early layers and propagate along separate channels, with only limited mixing with query or content representations [37]. In other words, the LLM appears to maintain different latent axes for role versus context, hinting at a structured internal organization of its ranking decisions.

These observations motivate our key research question: Do LLMs internally encode separable directions for role, relevance, and decision-making, and can these directions be isolated and manipulated to steer ranking behavior? If such latent concept vectors exist, they could provide a basis for systematically manipulating model activations to influence ranking outcomes. This shifts the focus from prompt engineering – often indirect and brittle – to direct activation-level control, enabling more precise and interpretable manipulation of model behavior.

To pursue this, we draw on activation steering methods: inference-time interventions that operate on hidden representations (activations) rather than model weights [2, 45]. In activation steering, one adds carefully chosen vectors to the model’s activations (e.g. at specific layers or tokens) to steer the output, for example, to better refuse harmful prompts [7] or reduce toxicity in LLM generations [33]. Crucially, this approach is post hoc, which means it works with a frozen model, offering flexible control without retraining. Recent work demonstrates that steering vectors can be constructed via contrastive methods or sparse autoencoders [10, 33, 34], and applied dynamically to elicit desired behaviors [40]. In our context, we aim to discover directions corresponding to role (policy) and relevance judgment, and then steer the LLM’s ranking outputs by intervening in these directions.

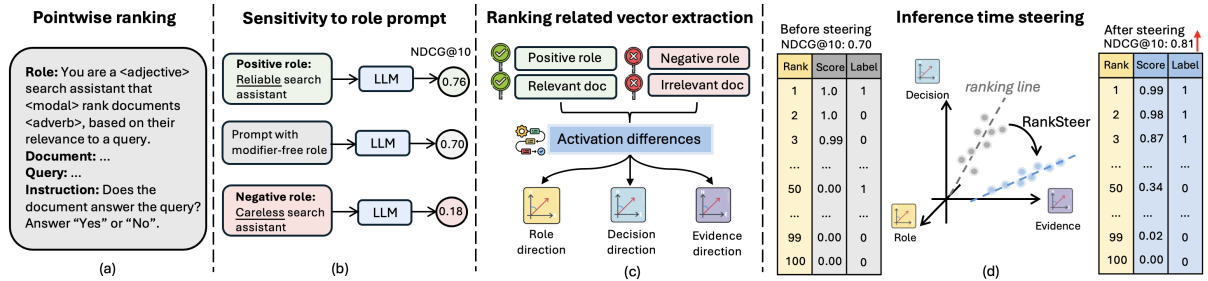


Figure 1: (a)(b) Pointwise LLM ranking prompt and its sensitivity to role phrasings. (c) Decomposing ranking decisions into separable decision, evidence, and role directions. (d) Performance gain after steering in inference time.

Unlike generation tasks with a single output, pointwise LLM ranking relies on repeated independent relevance judgments followed by a global sorting operation. This structure makes it possible to intervene not only on individual judgments, but also on how relevance scores are calibrated within the ranking process, providing a natural setting to disentangle *how* relevance decisions are made from *what* relevance signals are available.

Concretely, we characterize ranking decisions through three distinct and steerable directions in representation space, each capturing a different factor that influences how relevance judgments are produced (Figure 1(c)). First, we identify a **decision direction**, which defines how internal representations are mapped to relevance scores by the model’s output head. This direction is induced by the logit difference between the “Yes” and “No” predictions and serves as a global, input-agnostic axis governing pointwise relevance decisions. Second, we construct a *relevance judgment direction* using contrastive relevant and irrelevant documents that are consistent with the model’s existing ranking behavior. This direction captures how relevance is internally represented by the model at the hidden-state level. We then derive an **evidence direction** by removing the component of the relevance judgment direction that aligns with the decision axis. The resulting direction represents relevance-related signals present in the hidden space but not directly exploited by the decision head. Rather than altering the decision boundary, this evidence signal modulates how strongly relevance evidence is expressed during scoring. In addition, we extract a **role direction** from contrastive role-play prompts and explicitly orthogonalize it with respect to both the decision and evidence directions. This design ensures that role steering functions as a behavioral control signal, shaping the model’s decisiveness without injecting additional relevance information.

Building on these directions, we introduce a unified inference-time steering framework that jointly controls decision, evidence, and role signals through simple projection-based interventions (Figure 1(d)). This framework enables post-hoc calibration of the model’s ranking representations, improving ranking quality while preserving semantic fidelity. This paper makes the following contributions:

- We propose RankSteer, a post-hoc activation steering framework for zero-shot pointwise LLM ranking that disentangles and jointly controls decision, evidence, and role directions in the representation space, improving ranking performance

without modifying model weights or explicitly introducing cross-document comparisons.

- We demonstrate consistent ranking improvements across TREC DL 20 and BEIR benchmarks, showing that substantial ranking capacity remains under-utilized in zero-shot pointwise LLM rankers and can be recovered through activation-level calibration using only a small set of anchor queries.
- We provide a geometric and mechanistic analysis of ranking representations, revealing how steering reshapes ranking geometry by reducing dispersion and stabilizing decision structure.

2 Related Work

Zero-Shot Ranking. Pointwise LLM rankers prompt a model with a query and a single document to produce an independent relevance score, enabling simple and fully parallel inference. Representative approaches include query generation (QG) [28, 43], treating LLMs as query likelihood models [23], and relevance generation (RG), directly prompting the model to judge relevance and using label probabilities as scores. Variants such as RG-YN [15] and RG-S [41] perform ranking by using binary or graded relevance labels. Extensions like MCRanker [9] introduce multi-criteria prompting, while supervised models (e.g., MonoT5 [21], RankT5 [42]) require substantial labeled data and training. More recently, GCCP [17] improves pointwise ranking by introducing a global anchor for contrastive scoring. Despite their efficiency and ease of deployment, pointwise methods remain limited by calibration issues and under-utilization of internal ranking signals.

Comparative methods, including pairwise [18, 25], setwise [44] and listwise [19, 24, 31] prompting, improve ranking quality by explicitly introducing document comparisons. Pairwise approaches aggregate relative judgments across document pairs, while listwise methods directly generate ranked lists or permutations of candidates. These strategies often achieve stronger effectiveness than pointwise methods but suffer from high inference cost, limited parallelism, positional bias, and complex aggregation procedures [17]. In contrast to these approaches, RankSteer deliberately operates within the pointwise setting, without introducing cross-document comparisons or modifying the ranking protocol. Instead, we focus on a complementary question: how much ranking capacity remains under-utilized in zero-shot pointwise LLM rankers, and whether this capacity can be recovered through post-hoc activation steering. This positioning allows RankSteer to improve ranking performance

while preserving the simplicity, efficiency, and parallelism of pointwise inference.

Role-Play Prompting. Role-play prompting assigns an explicit role or persona to a language model, guiding its behavior and output style [29]. Modern LLMs exhibit strong role-playing abilities, enabling them to embody both human and abstract entities [13, 35]. In reasoning tasks, role-play prompting has been shown to act as an implicit form of chain-of-thought [38] guidance, improving performance without explicit reasoning steps [13]. For ranking tasks, zero-shot LLM rankers are highly sensitive to role-play instructions, which can lead to large performance variations [30, 37]. Recent causal intervention [20, 39] studies further show that role-play instructions are processed largely independently from query–document representations in the model’s hidden layers [37]. Building on these findings, our work moves beyond prompt-level manipulation by extracting and steering role-related activation directions, enabling post-hoc and interpretable control over ranking behavior.

Activation Steering. Activation steering has emerged as a light-weight and transparent paradigm for controlling LLM behavior without modifying model weights [2, 45]. The core premise is that many semantic concepts, behaviors, and decision patterns are encoded as approximately linear directions in the activation space, which can be identified and manipulated at inference time [22, 27]. In practice, steering directions are typically extracted using contrastive examples, probing classifiers, or sparse auto-encoders, and injected into hidden states to bias model outputs in a targeted manner [3, 10, 34]. This paradigm has been successfully applied across a wide range of tasks, including controlling persona and stylistic attributes [4], mitigating hallucinations [36], defending against jailbreak attacks [14, 40], and shaping reasoning behaviors [6]. For reasoning task, recent work has shown that role-playing behavior can be steered via internal activations using sparse autoencoders, leading to improved *reasoning* performance and highlighting the potential of activation-level control beyond surface-level prompt engineering [34].

However, the application of activation steering to *information retrieval* and ranking remains unexplored. Unlike generation or classification tasks, ranking quality emerges from aggregating many pointwise relevance judgments, raising open questions about whether and how internal steering can systematically improve ranking performance. This work addresses this gap by showing that relevance, decision, and role-play signals in pointwise LLM rankers can be disentangled and calibrated post hoc, enabling effective ranking improvements without modifying model parameters or introducing cross-document comparisons.

3 Methodology

We propose a multi-faceted activation steering framework for calibrating zero-shot pointwise LLM rankers that identifies three disentangled representation directions, decision, evidence, and role, and jointly controls their influence at inference time. Our method is illustrated in Figure 2.

3.1 Preliminaries

3.1.1 Pointwise Zero-Shot Reranking. We focus on the pointwise zero-shot document reranking paradigm, where a Large Language Model (LLM) is employed to independently evaluate the relevance of each query–document pair. Following established protocols in LLM-based retrieval [21], we adopt a binary Yes/No formulation [15]. Given a query q and a set of candidate documents $\mathcal{D} = \{d_1, d_2, \dots, d_n\}$, the model is prompted with a binary instruction to judge the relevance of each pair (q, d) , such as: “Does the passage answer the query? Answer ‘Yes’ or ‘No’.” Let Z_{yes} and Z_{no} denote the raw logits assigned to the tokens “Yes” and “No” respectively, at the final generation position. The relevance score $s(q, d)$ is defined as the softmax-normalized probability of the token “Yes”:

$$s(q, d) = \frac{\exp(Z_{\text{yes}})}{\exp(Z_{\text{yes}}) + \exp(Z_{\text{no}})} \quad (1)$$

The candidate documents are then ranked in descending order of $s(q, d)$. This formulation is particularly suitable for our study as it allows us to analyze relevance judgments directly through the model’s internal representations associated with the final token.

3.1.2 Activation Steering Framework. Activation steering typically involves two main steps:

Steering Vector Extraction. The steering process begins by identifying a steering vector $v^{(l)} \in \mathbb{R}^d$ that captures a desired attribute at layer l . A common practice involves using contrastive prompt pairs. For a given concept (e.g., relevance judgment), let X^+ be a set of positive examples (query and relevant documents) and X^- be a set of negative examples (query and irrelevant documents). The steering vector is computed as the mean difference between the hidden states $h_i^{(l)}$ of these pairs:

$$v^{(l)} = \frac{1}{n} \sum_{i=1}^n (h_{i+}^{(l)} - h_{i-}^{(l)}) \quad (2)$$

To ensure numerical stability and comparability across different layers, each steering vector is normalized to unit length such that $\|v^{(l)}\|_2 = 1$. In the context of pointwise LLM ranking, we start with a set of vectors $\mathcal{V} = \{v_{\text{relevance}}, v_{\text{role}}\}$. Here, v_{rel} represents relevance-judgment-related representation differences, while v_{role} captures role-induced behavioral biases.

Inference-Time Intervention. In this work, we focus on steering the last token hidden state, which typically aggregates the semantic information of the input sequence. For a transformer model with L layers, the intervention is applied at every layer during the forward pass. A basic form of activation steering modifies the hidden state by adding a steering vector scaled by a coefficient α :

$$\tilde{h}^{(l)} = h^{(l)} + \alpha \cdot v^{(l)} \quad (3)$$

While the steering vector is identified independently for each layer, its effect is accumulated as the modified signal propagates through the residual stream. A positive α shifts the model’s internal state toward the target concept, thereby modulating the output logits toward the desired distribution. More generally, activation steering can be implemented through projection-based interventions, allowing fine-grained control over how hidden states are modulated along specific vectors.

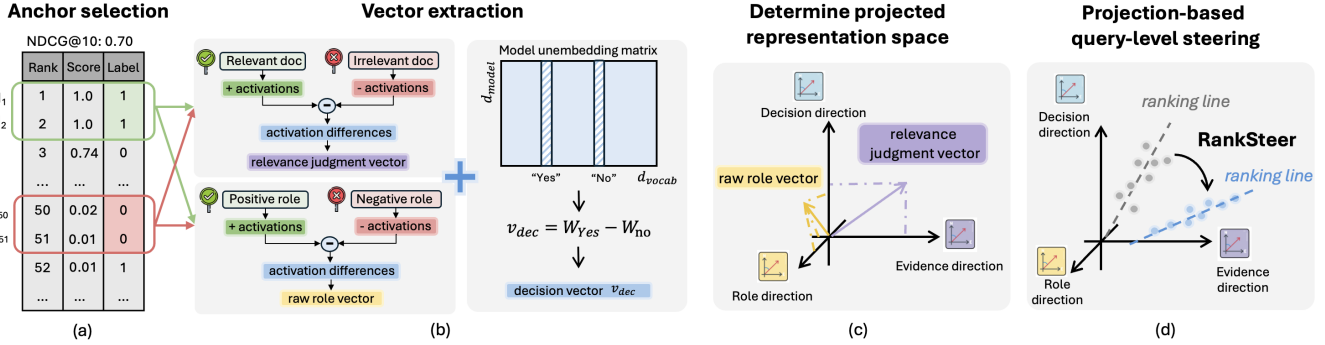


Figure 2: Overview of the RankSteer framework. (a) Selection of query–document anchors for constructing contrastive input pairs. (b) Extraction of ranking-related steering vectors from anchor data. (c) Construction of a projection-based representation space using the extracted vectors. (d) Inference-time, query-level activation steering via projections in the constructed space.

3.2 Constructing Steering Vectors

Our goal is to identify interpretable and disentangled directions that correspond to distinct factors influencing ranking. We move beyond simple contrastive extraction by explicitly separating the model’s output head bias from its internal semantic evidence.

3.2.1 Decision vector. The decision vector defines a global relevance axis induced by the model’s output head. In pointwise ranking, the model maps a high-dimensional hidden state to the logits of “Yes” and “No”. This mapping is governed by the model’s output embedding matrix $W \in \mathbb{R}^{V \times d}$. Let W_{yes} and W_{no} denote the weight rows corresponding to these tokens. We define the decision vector as the normalized difference:

$$v_{\text{dec}} = \frac{W_{\text{yes}} - W_{\text{no}}}{\|W_{\text{yes}} - W_{\text{no}}\|} \quad (4)$$

Unlike data-driven vectors, v_{dec} is input-agnostic and shared across all queries and documents. It represents the fixed geometric direction along which the final hidden state is projected to produce a judgment. Steering along this axis directly affects the model’s decisiveness without altering the underlying evidence representations.

3.2.2 Evidence vector. To extract a relevance signal that is consistent with the model’s existing ranking behavior with respect to a given dataset, we construct contrastive anchor pairs under both label and ranking constraints. Specifically, for a query q_i , we select n pairs of documents where the relevant document $d_{i,j}^+$ is ranked higher and the irrelevant document $d_{i,j}^-$ is ranked lower by the vanilla LLM. This ensures that the resulting contrast captures how the model currently distinguishes relevance, rather than representations associated with model errors or uncertainty. Let $h_{i,j}^{(l)+}$ and $h_{i,j}^{(l)-}$ denote the corresponding last-token hidden states at layer l . The raw relevance vector $v_{\text{rel}}^{(l)}$ is computed across m queries as:

$$v_{\text{rel}}^{(l)} = \frac{1}{m \cdot n} \sum_{i=1}^m \sum_{j=1}^n \left(h_{i,j}^{(l)+} - h_{i,j}^{(l)-} \right) \quad (5)$$

Disentanglement and Calibration. While $v_{\text{rel}}^{(l)}$ encodes relevance, a significant portion of this signal is already consumed by the decision head (v_{dec}). To isolate the residual relevance evidence that is present in the hidden states but not directly exploited for the final

“Yes/No” logit, we project $v_{\text{rel}}^{(l)}$ onto the orthogonal complement of the decision axis:

$$\tilde{v}_{\text{evid}}^{(l)} = v_{\text{rel}}^{(l)} - \langle v_{\text{rel}}^{(l)}, v_{\text{dec}} \rangle v_{\text{dec}} \quad (6)$$

The final evidence vector is obtained via normalization:

$$v_{\text{evid}}^{(l)} = \text{Norm}(\tilde{v}_{\text{evid}}^{(l)}) \quad (7)$$

The resulting evidence vector captures residual relevance information that is present in the model’s representations but not directly consumed by the logit-based decision mechanism. While the decision vector determines whether a document is judged relevant, the evidence vector reflects how strongly document content supports relevance in a way that is comparable across documents. As such, evidence serves as a calibration signal: steering along this direction modulates the contribution of under-utilized relevance cues without altering the underlying decision boundary.

3.2.3 Role vector. Beyond relevance signals derived from query–document content, LLMs are highly sensitive to high-level task framing and role-play instructions. Such role signals do not introduce new relevance evidence, but instead influence how the model applies its relevance judgment, acting as a form of policy-level control. To capture this effect, we construct a role vector that represents the impact of role-play on the model’s internal representations. To isolate role-specific signals, we construct contrastive role-play anchor pairs that differ only in their role instructions while keeping the query and document fixed. For a given query–document pair (q, d) , we prompt the model with a positive role instruction (e.g., “You are a reliable search assistant that can rank passages carefully, based on their relevance to a query.”) and a negative role instruction (e.g., “You are a careless search assistant that will rank passages wrongly, based on their relevance to a query.”). Let $h_{i,j,k}^{(l)\text{role}+}$ and $h_{i,j,k}^{(l)\text{role}-}$ be the hidden states for t contrastive role pairs. The raw role vector $v_{\text{role_raw}}^{(l)}$ is aggregated over m queries and n documents.

$$v_{\text{role_raw}}^{(l)} = \frac{1}{t} \frac{1}{n} \frac{1}{m} \sum_{k=1}^t \sum_{i=1}^n \sum_{j=1}^m \left(h_{i,j,k}^{(l)\text{role}+} - h_{i,j,k}^{(l)\text{role}-} \right) \quad (8)$$

To ensure that role steering operates independently of relevance judgments, we project $v_{\text{role_raw}}^{(l)}$ onto the orthogonal complement of

both the decision and evidence directions:

$$\tilde{v}_{\text{role}}^{(l)} = v_{\text{role_raw}}^{(l)} - (v_{\text{role_raw}}^{(l)} \cdot v_{\text{dec}}) v_{\text{dec}} - (v_{\text{role_raw}}^{(l)} \cdot v_{\text{evid}}^{(l)}) v_{\text{evid}}^{(l)} \quad (9)$$

The resulting vector is then normalized:

$$v_{\text{role}}^{(l)} = \text{Norm}(\tilde{v}_{\text{role}}^{(l)}) \quad (10)$$

After normalization, the resulting $v_{\text{role}}^{(l)}$ is orthogonal to both relevance-related axes. We do not attempt to analyze whether role and relevance are naturally disentangled. Instead, we explicitly construct independent directions to isolate the effect of role-play on relevance judgments from relevance evidence itself.

3.3 Layerwise Steering at Inference Time

We apply activation steering by intervening on the last-token hidden state $h^{(l)}$ at every layer. Unlike static prompting, this allows for fine-grained control over the model’s internal reasoning chain.

3.3.1 Projection Onto Steering Directions. Given the three unit steering vectors: decision vector v_{dec} , evidence vector $v_{\text{evid}}^{(l)}$, and role vector $v_{\text{role}}^{(l)}$, we first compute scalar projections of the hidden state:

$$p_{\text{dec}}^{(l)} = h^{(l)} \cdot v_{\text{dec}}, \quad p_{\text{evid}}^{(l)} = h^{(l)} \cdot v_{\text{evid}}^{(l)}, \quad p_{\text{role}}^{(l)} = h^{(l)} \cdot v_{\text{role}}^{(l)}. \quad (11)$$

These projections quantify how strongly the current representation aligns with the three directions at layer l .

3.3.2 Decision and Evidence Steering. We then apply relevance-oriented steering by adjusting the hidden state along the decision and evidence directions:

$$\tilde{h}^{(l)} = h^{(l)} - \alpha \cdot p_{\text{dec}}^{(l)} v_{\text{dec}} - \beta \cdot p_{\text{evid}}^{(l)} v_{\text{evid}}^{(l)} \quad (12)$$

where α and β control the scaling of the decision and evidence axes. Steering along v_{dec} affects the model’s global decisiveness, while steering along $v_{\text{evid}}^{(l)}$ modulates under-utilized relevance cues for better cross-document calibration.

3.3.3 Role-Gated Decision Steering. Role steering is applied in a gated manner to reflect its policy-level nature. Specifically, we use the role projection to compute a soft gating signal:

$$g^{(l)} = \sigma(p_{\text{role}}^{(l)}) \quad (13)$$

where $\sigma(\cdot)$ denotes the sigmoid function. This gate measures the activation strength of role-related features at layer l . We then modulate the decision-direction steering conditioned on this gate:

$$h'^{(l)} = \tilde{h}^{(l)} - \gamma \cdot g^{(l)} \cdot p_{\text{dec}}^{(l)} v_{\text{dec}} \quad (14)$$

where γ is the role modulation coefficient.

By design, role steering does not inject relevance information nor directly alter evidence representations. Instead, it adaptively scales the strength of decision steering based on the role signal, influencing how decisively the model applies its relevance judgment.

3.3.4 Final Scoring. After steering all layers, the final hidden state is passed to the output head to compute relevance logits, from which pointwise relevance scores are derived as described in Section 3.1.1. All hyperparameters α , β , and γ are fixed at inference time and tuned empirically on an external validation set.

4 Experiments

4.1 Experimental Setup

4.1.1 Datasets and Evaluation Metrics. We construct steering vectors and evaluate the effectiveness of our method on two widely used IR benchmarks: TREC Deep Learning (DL) [5] and BEIR [32]. TREC DL is a dense-relevance benchmark with high-quality graded judgments, making it well suited for constructing reliable relevance and role-play anchor data. To extract stable steering vectors, we require documents that are not only labeled as relevant or irrelevant, but also ranked consistently with the model’s existing behavior. Therefore, we use a small subset of queries from TREC DL 2019 to construct relevance and role-play anchor inputs, and use the remaining queries from TREC DL 2019 as a validation set to tune the steering hyperparameters α , β , and γ . We evaluate in-distribution generalization on TREC DL 2020, which shares the same document corpus as DL 2019 but contains disjoint queries. To assess out-of-distribution generalization, we further evaluate on eight datasets from BEIR, following prior work: Covid, Touche, Signal, News, SciFact, Robust04, DBPedia, and NFCorpus. We report nDCG@10 as the primary evaluation metric. In addition, when analyzing the effects of individual steering directions, we also report MRR@10, MAP, and binary accuracy. Binary accuracy measures whether an independent relevance judgment is correct in pointwise ranking. In the Yes/No setting, we compute the relevance score as the normalized likelihood of generating “Yes” relative to “No”, and classify predictions using a threshold of 0.5.

4.1.2 Baselines. We compare RankSteer against a diverse set of state-of-the-art baselines for zero-shot LLM ranking, covering pointwise, pairwise, setwise, and listwise paradigms. Among pointwise baselines, **QG** [28] scores documents based on query generation likelihood. **RG-YN** [15] uses the probability of generating “Yes” relative to “No” as the relevance score. **RG-S(0-k)** [41] extends RG-YN by prompting the model to rate relevance on a discrete scale; following prior work, we set $k = 4$. **GCCP** [17] incorporates global-consistent pairwise comparisons into a pointwise framework. We adopt **PAGC-YG** [17], a post-aggregation technique, to combine GCCP with RG-YN. For pairwise ranking, we compare against **PRP** [18], which produces relative relevance labels for document pairs and derives a ranking via heapsort. **Setwise** [44] methods leverage sorting-based selection over document sets to focus on top-k ranking by repeatedly identifying the most relevant candidate. For listwise ranking, we compare against **RankGPT** [31], which generates a global ordering over candidate documents using a sliding-window listwise prompting strategy. To highlight the sensitivity of LLM rankers to role-play prompts, we also report results for **RG-YN_role**, which augments RG-YN with a neutral role-play description [37]. Based on this setting, we evaluate **RankSteer**, which applies post-hoc activation steering to RG-YN_role without modifying prompts or model parameters.

4.1.3 Implementation Details. We use Pyserini [16] to retrieve top-100 BM25 candidates for all datasets. We reproduce all baselines using decoder-only LLMs for consistency. Our experiments include Llama-3.1-8B-Instruct [8], Qwen2.5-7B-Instruct [26], and Mistral-7B-Instruct-v0.3 [1, 12]. To construct relevance anchor inputs, we select $m = 5$ queries from TREC DL 2019. For each query, we

Table 1: Comparison of our RankSteer method to other pointwise ranking methods, in terms of nDCG@10. RG-YN_role is the baseline ranker with a neutral role, without steering. All LLMs are instruction-tuned versions. The best result per dataset and LLM is marked with boldface; underline indicates the second-best result.

		TREC DL		BEIR								
		Methods	dl20	covid	touche	signal	news	scifact	robust04	dbpedia	nfcorpus	Avg
LLaMa3.1-8B	BM25	0.4796	0.5947	0.4422	0.3304	0.3952	0.6789	0.4070	0.3180	0.3218	0.4360	
	QG	0.3498	0.6925	0.2205	0.1015	0.4221	0.6041	0.4508	0.2817	0.3506	0.3905	
	RG-YN	0.6109	0.7261	0.2264	0.2482	0.3665	0.5677	0.5046	0.3093	0.3563	0.4131	
	RG-S(0,4)	0.5190	<u>0.7902</u>	0.2205	0.2637	0.4451	0.6241	0.5039	<u>0.3666</u>	0.3646	0.4473	
	PAGC-YG	0.6193	0.7534	<u>0.2424</u>	0.2586	0.4503	0.6485	0.5199	0.3420	0.3596	0.4468	
	RG-YN_role	<u>0.6230</u>	0.7792	0.2227	<u>0.2661</u>	<u>0.4456</u>	0.6606	0.5321	0.3574	<u>0.3715</u>	0.4544	
	RankSteer	0.6461	0.7863	0.2445	0.2779	0.4462	0.6498	<u>0.5207</u>	0.3752	0.3732	0.4588	
Qwen2.5-7B	QG	0.3982	0.6463	0.2190	0.0922	0.2533	0.3499	0.3617	0.2530	0.2845	0.3075	
	RG-YN	0.6203	0.6780	0.2025	0.2305	0.3040	0.2395	0.3484	0.2733	0.3106	0.3234	
	RG-S(0,4)	0.6059	0.7814	0.2333	0.2661	0.4490	0.6261	0.4756	<u>0.3618</u>	<u>0.3599</u>	0.4441	
	PAGC-YG	<u>0.6500</u>	0.7395	0.2413	<u>0.2761</u>	0.3772	0.4632	0.4488	0.3525	0.3552	0.4067	
	RG-YN_role	0.6156	0.7212	0.1985	0.2249	0.3048	0.2398	0.3691	0.2909	0.3183	0.3334	
	RankSteer	0.6594	<u>0.7678</u>	<u>0.2356</u>	0.2793	<u>0.3807</u>	0.4133	0.4338	0.3749	0.3697	0.4069	
	Mistral-7B	0.4287	0.6621	0.2277	0.1010	0.3048	0.4816	0.3506	0.3075	0.3019	0.3422	
Mistral-7B	RG-YN	0.4897	0.7315	0.1976	0.2243	0.3963	0.5143	0.4760	0.2791	0.3335	0.3941	
	RG-S(0,4)	0.5491	<u>0.7892</u>	0.2468	<u>0.2679</u>	0.4678	0.6324	0.4856	<u>0.3672</u>	<u>0.3512</u>	0.4510	
	PAGC-YG	<u>0.5522</u>	0.7775	0.2212	0.2586	0.3949	0.4476	<u>0.4894</u>	0.3307	0.3338	0.4067	
	RG-YN_role	0.5082	0.7136	0.1998	0.2268	0.4192	0.5304	0.4884	0.2954	0.3401	0.4017	
	RankSteer	0.6355	0.8019	<u>0.2254</u>	0.2877	0.4441	0.5664	0.5123	0.3965	0.3623	0.4496	

choose $n = 10$ relevant documents ranked high (closest to rank 1) and $n = 10$ irrelevant documents ranked relatively low (rank 50–60) under the baseline zero-shot ranker. This ensures that the extracted relevance judgment vectors are consistent with the model’s existing ranking behavior. To construct role-play anchor inputs, we use $t = 3$ pairs of positive and negative role-play instructions, selected based on their observed impact on ranking performance in a prior work [37]. We use the remaining 38 queries from TREC DL 2019 to tune the steering hyperparameters α , β , and γ . Once tuned, these parameters are fixed and applied to TREC DL 2020 and all BEIR datasets. Since the construction of anchor inputs involves random query selection from TREC DL 2019, which may introduce variability, we further mitigate this effect by performing a multi-fold selection procedure. Specifically, we split TREC DL 2019 into 9 partitions, where each of the first 8 partitions uses a distinct set of 5 queries as anchor data. For each partition, we compute a corresponding anchor vector and evaluate its performance on the validation queries. We then select the anchor vector from the partition that achieves the best validation performance gain as the final vector used in all subsequent experiments. We use $(\alpha = 0.60, \beta = 0.16, \gamma = 0.04)$ for Llama, $(0.25, -0.06, 0.08)$ for Qwen and $(0.40, 0.00, 0.06)$ for Mistral. All experiments are conducted on a workstation equipped with four NVIDIA L40S GPUs (48GB memory each).

4.2 Experimental Results

4.2.1 Comparison with pointwise methods. We compare RankSteer with representative and state-of-the-art pointwise LLM ranking methods in Table 1 and summarize three main observations. First, RankSteer achieves the strongest performance among pointwise methods on TREC DL 2020, which shares the same document corpus as TREC DL 2019 and serves as an in-distribution evaluation set. Notably, using only five anchor queries from DL19, RankSteer improves the nDCG@10 of Mistral-7B-Instruct-v0.3 from 0.5082 to 0.6355 on unseen DL20 queries, demonstrating that effective steering directions can be extracted from a very small anchor set and transferred to new queries within the same domain.

Second, the effectiveness of RankSteer varies across backbone models, with Llama-3.1-8B-Instruct consistently serving as the best backbone for steering. On this model, RankSteer yields the largest and most stable improvements, outperforming other pointwise baselines on the majority of datasets. On SciFact and Robust04, a simple neutral role prompt (RG-YN_role) achieves slightly higher nDCG, although RankSteer remains competitive. In contrast, RankSteer yields smaller gains on Qwen2.5-7B-Instruct and moderate improvements on Mistral-7B-Instruct-v0.3, while still achieving the best or second-best performance on more than half of the evaluated datasets for both models.

Finally, across all models and datasets, adding a neutral role description to the RG-YN baseline generally improves ranking performance and can occasionally match the best results on Llama-3.1-8B-Instruct.

Table 2: Comparison of our RankSteer method to other ranking methods, in terms of nDCG@10. The best result per dataset and LLM is marked with boldface; underline indicates the second-best result.

		TREC DL			BEIR						Avg	
		Methods	dl20	covid	touche	signal	news	scifact	robust04	dbpedia		
	BM25	BM25	0.4796	0.5947	0.4422	0.3304	0.3952	0.6789	0.4070	0.3180	0.3218	0.4360
LLaMa3.1-8B	pairwise	pairwise	0.6098	0.7835	0.2578	0.2891	0.4700	0.7032	0.5115	0.3800	0.3658	0.4701
	setwise	setwise	0.6112	0.7789	0.2470	0.2946	0.4614	0.6808	0.4965	0.3774	0.3494	0.4608
	listwise	listwise	0.6587	0.8112	0.2744	0.3107	0.4833	0.6762	0.5201	0.4189	0.3690	0.4830
	RankSteer	RankSteer	<u>0.6461</u>	<u>0.7863</u>	0.2445	0.2779	0.4462	0.6498	0.5207	0.3752	0.3732	0.4588
Qwen2.5-7B	pairwise	pairwise	0.6590	0.7989	0.3038	0.3111	0.4968	0.6968	0.5415	0.4134	0.3796	0.4927
	setwise	setwise	0.6531	<u>0.8099</u>	0.2883	0.2999	0.4788	0.6800	0.5210	0.4074	0.3786	0.4830
	listwise	listwise	0.6785	0.8234	0.3184	0.3363	0.4989	0.7107	0.5438	0.4324	0.3905	0.5068
	RankSteer	RankSteer	<u>0.6594</u>	0.7678	0.2356	0.2793	0.3807	0.4133	0.4338	0.3749	0.3697	0.4069
Mistral-7B	pairwise	pairwise	0.5559	0.7966	<u>0.3099</u>	<u>0.3036</u>	0.4854	0.6655	0.4981	0.3354	0.3541	0.4696
	setwise	setwise	0.6171	0.8160	0.2879	0.2919	0.4520	0.6260	0.4813	0.3953	0.3615	0.4640
	listwise	listwise	0.6491	0.8006	0.3521	0.3268	0.5092	<u>0.6584</u>	0.5359	0.4425	0.3713	0.4996
	RankSteer	RankSteer	<u>0.6355</u>	<u>0.8019</u>	0.2254	0.2877	0.4441	0.5664	0.5123	0.3965	0.3623	0.4496

4.2.2 Effectiveness and efficiency compared with other methods. Table 2 compares RankSteer with representative pairwise, setwise, and listwise ranking methods, and BM25. While comparative methods such as pairwise and listwise prompting generally achieve stronger effectiveness by explicitly introducing document comparisons, RankSteer operates under a strictly pointwise setting without access to cross-document information. As a result, it is not expected to consistently outperform listwise methods. Instead, our results demonstrate that, even under this constrained setting, substantial ranking improvements can be obtained through post-hoc calibration alone. In particular, RankSteer achieves performance comparable to strong comparative methods on TREC DL 2020 and occasionally matches or surpasses them on several BEIR datasets. From a computational perspective, RankSteer retains the same lowest time complexity as standard pointwise ranking, incurring only a constant-time ($O(1)$) for activation steering. In contrast, comparative methods require additional document interactions, leading to $O(N)$ complexity for listwise approaches and $O(\log N)$ for heap-based pairwise and setwise methods.¹ Together, these results suggest that a significant portion of the performance gap between pointwise and comparative methods stems from how internal relevance signals are utilized and scaled, rather than from the absence of explicit cross-document comparisons. RankSteer therefore offers a favorable trade-off, recovering much of this gap while preserving the simplicity, efficiency, and full parallelism of pointwise inference.

4.2.3 Ablation Study of Steering Directions. We conduct an ablation study to analyze the contributions of individual steering directions and their combinations. Table 3 reports validation results on a randomly selected partition of TREC DL 2019 using Llama-3.1-8B-Instruct. We find that single-direction steering yields limited

¹Long et al.[17] distinguish between time complexity and number of LLM calls in the analysis of the complexity of ranking methods. Here we focus on time complexity.

Table 3: Ablation study of activation steering directions on a TREC DL 2019 validation fold with LLaMA-3.1-8B-Instruct. BA indicates binary accuracy.

Vector	nDCG@10	MRR@10	MAP	BA
-	0.6800	0.8985	0.3656	0.7665
v_{dec}	0.6963	0.9193	0.3673	0.7457
v_{evid}	0.6843	0.9020	0.3662	0.7665
$v_{dec} + v_{evid}$	<u>0.7061</u>	<u>0.9386</u>	<u>0.3701</u>	0.7625
$v_{dec} + v_{role}$	0.7029	0.9456	0.3674	0.7486
$v_{dec} + v_{role} + v_{evid}$	0.7102	0.9342	0.3712	0.7641

but distinct effects. Decision-only steering (v_{dec}) substantially improves ranking metrics but reduces BA, reflecting a rescaling of the decision scores. In contrast, evidence-only steering (v_{evid}) produces smaller ranking gains while preserving BA, indicating that it injects relevance information without directly altering the decision boundary. Secondly, combining directions leads to larger improvements. Steering with decision and evidence ($v_{dec} + v_{evid}$) clearly outperforms all single-direction settings, demonstrating the complementarity of these signals. Steering with decision and role ($v_{dec} + v_{role}$) also improves ranking, particularly MRR, but is less effective than evidence-based steering in terms of nDCG and MAP. Finally, jointly steering along all three directions ($v_{dec} + v_{evid} + v_{role}$) achieves the best overall ranking performance, yielding the highest nDCG and MAP while keeping BA close to the baseline. This suggests that decision, evidence, and role directions contribute complementary effects to ranking quality without destabilizing pointwise relevance judgments.

4.2.4 Sensitivity to Anchor Query Set. To assess sensitivity to anchor query selection, we construct steering vectors from eight disjoint partitions of TREC DL 2019, each containing five queries,

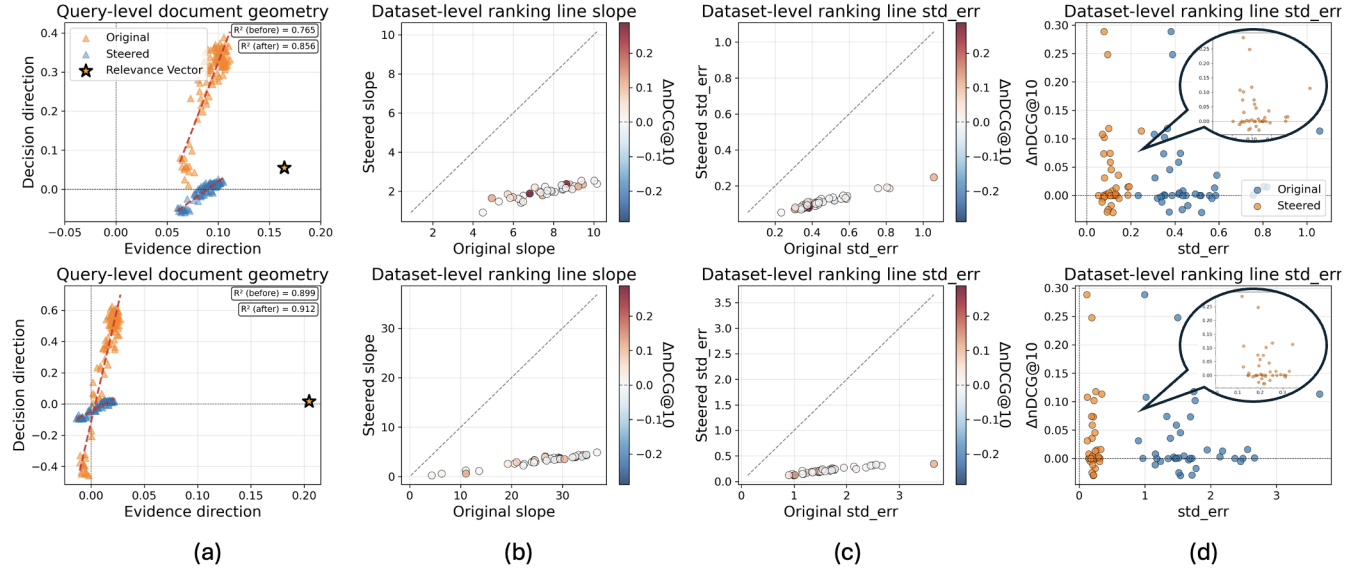


Figure 3: Geometric interpretability of RankSteer at Layers 16 (top) and 19 (bottom) of Llama3.1-8B-Instruct. (a) Query-level document representations projected onto the decision–evidence plane, illustrating linear ranking geometry. (b) and (c) Dataset-level distributions of the slope and standard error of query-specific ranking lines before and after steering. (d) A complementary view of (c), highlighting how steering redistributes query-level ranking dispersion in relation to changes in nDCG.

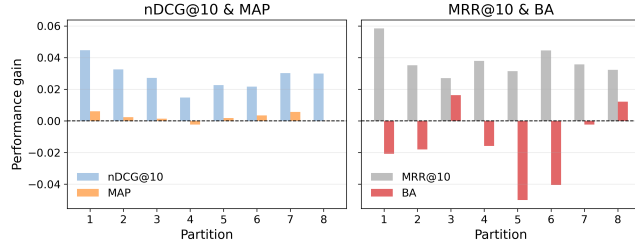


Figure 4: Sensitivity to anchor query set. Performance gain after steering across eight anchor sets (5 queries) of TREC DL 19 using Llama-3.1-8B-Instruct.

and tune hyperparameters within each partition. Figure 4 summarizes the resulting performance changes. Steering consistently improves ranking quality across all partitions: both nDCG@10 and MRR@10 increase for all eight anchor sets, with gains of comparable magnitude, indicating that effective steering directions can be reliably extracted from different small anchor subsets. MAP shows smaller variations, with modest improvements in six partitions and slight decreases in two partitions, while BA shows larger fluctuations across partitions, with most partitions exhibiting a decrease. This behavior is expected, as steering rescales decision scores and can shift the optimal threshold for pointwise Yes/No judgments, without necessarily degrading ranking quality. Overall, while the magnitude of improvement varies with the anchor set, the direction of the effect remains stable. RankSteer is therefore only moderately sensitive to anchor selection and does not depend on a carefully chosen or exceptional anchor set to be effective.

4.2.5 Effect of Anchor Query Counts. To examine how many anchor queries are required to extract stable steering vectors, we conduct

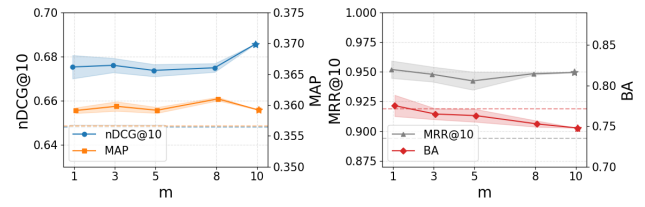


Figure 5: Effect of anchor query counts on TREC DL 2019 with Llama3.1-Instruct-8B. The horizontal dotted line is the baseline without model steering. For $m = 10$, there is only one set of queries and therefore a single measurement.

an analysis on TREC DL 2019. We fix 33 queries as a validation set and use the remaining 10 queries as an anchor pool. From this pool, we randomly sample $m \in \{1, 3, 5, 8, 10\}$ queries to construct steering vectors, repeating the process five times and reporting the mean and standard deviation in Figure 5. Overall, ranking performance is relatively insensitive to the number of anchor queries. Both nDCG@10 and MRR@10 remain stable across different values of m , and consistently outperform the no-steering baseline. Even a single anchor query can yield competitive average performance, but exhibits noticeably higher variance, indicating reduced stability. MAP shows slightly larger fluctuations, peaking around $m = 8$, while binary accuracy gradually decreases as m increases. This behavior reflects a trade-off between stronger ranking calibration and threshold-based pointwise accuracy, as steering increasingly rescales decision scores. Considering both performance stability and variance, we adopt $m = 5$ anchor queries in our main experiments as a balanced setting that provides robust gains without introducing unnecessary variance or calibration side effects.

Table 4: Comparison of steering and fine-tuned model on the same anchor set (5 queries) using LLaMA3.1-8B-Instruct.

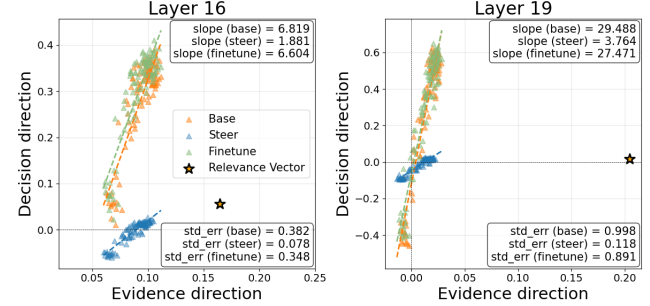
Model	nDCG@10	MRR@10	MAP	BA
Vanilla	0.6715	0.9079	0.3807	0.7694
Fine-tuned	0.6773	0.9430	0.3783	0.7650
Steered	0.7040	0.9430	0.3831	0.7513

4.2.6 Interpretability from the geometric perspective. Since role-play primarily modulates the decision mechanism rather than document content, we analyze ranking behavior in the two-dimensional space spanned by the decision and evidence directions. Figure 3 visualizes ranking geometry at both the query and dataset levels.

What is being steered? Figure 3(a) shows query-level document representations projected onto the decision–evidence plane. For a given query, document representations exhibit an approximately linear arrangement, which we refer to as a *ranking line*. This linear structure is consistently observable both before and after steering. Rather than changing the existence of the ranking line, steering modifies its statistical properties. In particular, document representations become more concentrated, with reduced spread along the decision direction. This indicates that steering affects how strongly documents are separated by the decision mechanism, while preserving the underlying ranking geometry induced by the query. This effect is more clearly observed at the dataset level: Figures 3(b) and (c) report the slope and standard error of fitted ranking lines across queries. For layers where ranking geometry is well-formed (approximately Layers 15–31), steering consistently reduces both slope and dispersion. We report representative results from Layers 16 and 19. These changes indicate that steering reduces the dominance of the decision direction relative to the evidence direction, allowing document representations to align more closely with evidence-supported relevance signals. As a result, ranking structures become more coherent and stable across queries.

The Triangular Gain Region. Figure 3(d) shows the relationship between ranking dispersion (standard error of the ranking line) and changes in ranking quality (Δ nDCG), before and after steering. In both cases, queries form an approximately triangular-shaped region. Steering does not change the shape of this region. Instead, it shifts queries horizontally toward lower dispersion values, while the overall triangular pattern remains the same. This indicates that steering reduces ranking dispersion but does not fundamentally alter how dispersion constrains ranking outcomes. The triangular region reflects an inherent property of the model’s ranking behavior: queries with high dispersion exhibit more limited changes in ranking quality, whereas queries with lower dispersion allow larger – but still bounded – changes. In this sense, the triangle describes how much a query’s ranking can change, not whether it will improve. Overall, steering improves ranking by moving queries into lower-dispersion regimes within an existing ranking geometry, rather than introducing new ranking behaviors or changing the underlying ranking mechanism.

Comparison with fine-tuning. To compare activation steering with fine-tuning, we use the same anchor set as in Figure 3 and use the same 5 anchor queries to fine-tune Llama-3.1-8B-Instruct with

**Figure 6: Comparison of query-level document representations under steering and fine-tuning on Layer 16 and 19.**

LoRA [11]. Both approaches are evaluated on the same validation set (Table 4). With identical anchor data, fine-tuning yields a modest improvement in nDCG@10, increasing from 0.6715 to 0.6773, while substantially improving MRR@10. In contrast, activation steering achieves a much larger gain in nDCG@10, reaching 0.7040, while matching the fine-tuned model in MRR@10, all without updating model weights. MAP shows a small improvement under steering, whereas binary accuracy decreases slightly, consistent with the rescaling of decision scores introduced by steering. Figure 6 further contrasts the geometric effects of the two approaches. Fine-tuned representations largely preserve the ranking geometry of the base model: query-specific ranking lines maintain similar orientation, with only moderate reductions in slope and dispersion. Activation steering, by comparison, induces a stronger geometric effect, substantially compressing both slope and dispersion and yielding tighter clustering along the decision direction while remaining close to the original ranking manifold.

Taken together, these results highlight the sample efficiency advantage of activation steering in low-resource settings. With only five anchor queries, steering produces markedly larger ranking gains than fine-tuning, suggesting that directly manipulating activation geometry can recover under-utilized ranking capacity more effectively than parameter updates when supervision is scarce.

5 Conclusion

In this paper, we propose RankSteer, a post-hoc activation steering method for pointwise LLM rankers. By characterizing ranking behavior through three steerable directions – decision, evidence, and role – we show that ranking performance can be effectively calibrated at inference time through simple projection-based interventions, without modifying model weights or introducing cross-document comparisons. We evaluated RankSteer on TREC-DL 2020 and the BEIR benchmarks with three backbone LLMs, constructing steering vectors from only five anchor queries drawn from an external dataset. Our results show that RankSteer outperforms state-of-the-art pointwise LLM ranking methods. RankSteer with Llama3.1-8B as backbone model is also competitive to pairwise, setwise, and listwise methods on several datasets. While listwise methods achieve the strongest average effectiveness, they incur substantially higher computational cost; in contrast, RankSteer preserves the inference complexity of standard pointwise ranking. Overall,

activation steering provides an efficient post-hoc calibration mechanism for pointwise LLM rankers, recovering under-utilized ranking capacity with far fewer labeled queries than fine-tuning. For future work, the development of activation steering methods for other ranking paradigms and retrieval settings should be investigated.

Acknowledgments

References

- [1] Mistral AI. 2024. Mistral-7B-Instruct-v0.3 Model Card. <https://huggingface.co/mistralai/Mistral-7B-Instruct-v0.3>. Accessed 2025.
- [2] Lukasz Bartoszcz, Sarthak Munshi, Bryan Sukidi, Jennifer Yen, Zejia Yang, David Williams-King, Linh Le, Kosi Asuzu, and Carsten Maple. 2025. Representation Engineering for Large-Language Models: Survey and Research Challenges. *arXiv preprint arXiv:2502.17601* (2025).
- [3] Reza Bayat, Ali Rahimi-Kalahrudi, Mohammad Pezeshki, Sarath Chandar, and Pascal Vincent. 2025. Steering large language model activations in sparse spaces. *arXiv preprint arXiv:2503.00177* (2025).
- [4] Runjin Chen, Andy Ardit, Henry Sleight, Owain Evans, and Jack Lindsey. 2025. Persona vectors: Monitoring and controlling character traits in language models. *arXiv preprint arXiv:2507.21509* (2025).
- [5] Nick Craswell, Bhaskar Mitra, Emine Yilmaz, Daniel Campos, Jimmy Lin, Ellen M Voorhees, and Ian Soboroff. 2025. Overview of the TREC 2022 deep learning track. *arXiv preprint arXiv:2507.10865* (2025).
- [6] Yi Fang, Wenjie Wang, Mingfeng Xue, Boyi Deng, Fengli Xu, Dayiheng Liu, and Fuli Feng. 2026. Controllable LLM Reasoning via Sparse Autoencoder-Based Steering. *arXiv:2601.03595* [cs.AI] <https://arxiv.org/abs/2601.03595>
- [7] Shaona Ghosh, Amrita Bhattacharjee, Yftah Ziser, and Christopher Parisien. 2025. A Simple Yet Effective Method for Non-Refusing Context Relevant Fine-grained Safety Steering in LLMs. In *Proceedings of the 2025 Conference on Empirical Methods in Natural Language Processing*, Christos Christodoulopoulos, Tanmoy Chakraborty, Carolyn Rose, and Violet Peng (Eds.). Association for Computational Linguistics, Suzhou, China, 35128–35148. doi:10.18653/v1/2025.emnlp-main.1781
- [8] Aaron Grafftfiori, Abhimanyu Dubey, Abhinav Jauhri, Abhinav Pandey, Abhishek Kadian, Ahmad Al-Dahle, Aiesha Letman, Akhil Mathur, Alan Schelten, Alex Vaughan, et al. 2024. The llama 3 herd of models. *arXiv preprint arXiv:2407.21783* (2024).
- [9] Fang Guo, Wenyu Li, Honglei Zhuang, Yun Luo, Yafu Li, Le Yan, Qi Zhu, and Yue Zhang. 2025. Mcranker: Generating diverse criteria on-the-fly to improve pointwise ILM rankers. In *Proceedings of the Eighteenth ACM International Conference on Web Search and Data Mining*. 944–953.
- [10] Yihui Hong, Meng Cao, Dian Zhou, Lei Yu, and Zhijing Jin. 2025. The Reasoning-Memorization Interplay in Language Models Is Mediated by a Single Direction. In *Findings of the Association for Computational Linguistics: ACL 2025*, Wanxiang Che, Joyce Nabende, Ekaterina Shutova, and Mohammad Taher Pilehvar (Eds.). Association for Computational Linguistics, Vienna, Austria, 21565–21585. doi:10.18653/v1/2025.findings-acl.1111
- [11] Edward J Hu, Yelong Shen, Phillip Wallis, Zeyuan Allen-Zhu, Yuanzhi Li, Shean Wang, Lu Wang, Weizhu Chen, et al. 2022. Lora: Low-rank adaptation of large language models. *ICLR* 1, 2 (2022), 3.
- [12] Albert Q. Jiang, Alexandre Sablayrolles, Arthur Mensch, Chris Bamford, Devendra Singh Chaplot, Diego de las Casas, Florian Bressand, Gianna Lengyel, Guillaume Lampe, Lucile Saulnier, Lélio Renard Lavaud, Marie-Anne Lachaux, Pierre Stock, Thibaut Lavril, Thomas Wang, Timothée Lacroix, and William El Sayed. 2023. Mistral 7B. *arXiv:2310.06825* [cs.CL] <https://arxiv.org/abs/2310.06825>
- [13] Aobo Kong, Shiwani Zhao, Hao Chen, Qicheng Li, Yong Qin, Ruiqi Sun, Xin Zhou, Enzhi Wang, and Xiaohang Dong. 2024. Better zero-shot reasoning with role-play prompting. In *Proceedings of the 2024 Conference of the North American Chapter of the Association for Computational Linguistics: Human Language Technologies (Volume 1: Long Papers)*. 4099–4113.
- [14] Tianlong Li, Zhenghua Wang, Wenhao Liu, Muling Wu, Shihan Dou, Changze Lv, Xiaohua Wang, Xiaoqing Zheng, and Xuanjing Huang. 2025. Revisiting Jail-breaking for Large Language Models: A Representation Engineering Perspective. In *Proceedings of the 31st International Conference on Computational Linguistics*, Owen Rambow, Leo Wanner, Marianna Apidianaki, Henda Al-Khalifa, Barbara Di Eugenio, and Steven Schockaert (Eds.). Association for Computational Linguistics, Abu Dhabi, UAE, 3158–3178. <https://aclanthology.org/2025.coling-main.212/>
- [15] Percy Liang, Rishi Bommasani, Tony Lee, Dimitris Tsipras, Dilara Soylu, Michihiro Yasunaga, Yian Zhang, Deepak Narayanan, Yuhuai Wu, Ananya Kumar, et al. 2022. Holistic evaluation of language models. *arXiv preprint arXiv:2211.09110* (2022).
- [16] Jimmy Lin, Xueguang Ma, Sheng-Chieh Lin, Jheng-Hong Yang, Ronak Pradeep, and Rodrigo Nogueira. 2021. Pyserini: A Python Toolkit for Reproducible Information Retrieval Research with Sparse and Dense Representations. In *Proceedings of the 44th Annual International ACM SIGIR Conference on Research and Development in Information Retrieval (SIGIR 2021)*. 2356–2362.
- [17] Kehan Long, Shasha Li, Chen Xu, Jintao Tang, and Ting Wang. 2025. Precise Zero-Shot Pointwise Ranking with LLMs through Post-Aggregated Global Context Information. In *Proceedings of the 48th International ACM SIGIR Conference on Research and Development in Information Retrieval*. 2384–2394.
- [18] Jian Luo, Xuanang Chen, Ben He, and Le Sun. 2024. Prp-graph: Pairwise ranking prompting to ILMs with graph aggregation for effective text re-ranking. In *Proceedings of the 62nd Annual Meeting of the Association for Computational Linguistics (Volume 1: Long Papers)*. 5766–5776.
- [19] Xueguang Ma, Xinyu Zhang, Ronak Pradeep, and Jimmy Lin. 2023. Zero-shot listwise document reranking with a large language model. *arXiv preprint arXiv:2305.02156* (2023).
- [20] Kevin Meng, David Bau, Alex Andonian, and Yonatan Belinkov. 2022. Locating and editing factual associations in gpt. *Advances in neural information processing systems* 35 (2022), 17359–17372.
- [21] Rodrigo Nogueira, Zhiyong Jiang, Ronak Pradeep, and Jimmy Lin. 2020. Document ranking with a pretrained sequence-to-sequence model. In *Findings of the Association for Computational Linguistics: EMNLP 2020*. 708–718.
- [22] Kiho Park, Yo Joong Choe, and Victor Veitch. 2023. The linear representation hypothesis and the geometry of large language models. *arXiv preprint arXiv:2311.03658* (2023).
- [23] Jay M Ponte and W Bruce Croft. 2017. A language modeling approach to information retrieval. In *ACM SIGIR Forum*, Vol. 51. ACM New York, NY, USA, 202–208.
- [24] Ronak Pradeep, Sahel Sharifmoghaddam, and Jimmy Lin. 2023. Rankvicut: Zero-shot listwise document reranking with open-source large language models. *arXiv preprint arXiv:2309.15088* (2023).
- [25] Zhen Qin, Rolf Jagerman, Kai Hui, Honglei Zhuang, Junru Wu, Le Yan, Jiaming Shen, Tianqi Liu, Jialu Liu, Donald Metzler, et al. 2024. Large language models are effective text rankers with pairwise ranking prompting. In *Findings of the Association for Computational Linguistics: NAACL 2024*. 1504–1518.
- [26] Qwen, ;, An Yang, Baosong Yang, Beichen Zhang, Binyuan Hui, Bo Zheng, Bowen Yu, Chengyuan Li, Dayiheng Liu, Fei Huang, Haoran Wei, Huan Lin, Jian Yang, Jianhong Tu, Jianwei Zhang, Jianxin Yang, Jiaxi Yang, Jingren Zhou, Junyang Lin, Kai Dang, Keming Lu, Keqin Bao, Kexin Yang, Le Yu, Mei Li, Mingfeng Xue, Pei Zhang, Qin Zhu, Rui Men, Runji Lin, Tianhao Li, Tianyi Tang, Tingyu Xia, Xingzhang Ren, Xuancheng Ren, Yang Fan, Yang Su, Yichang Zhang, Yu Wan, Yuqiong Liu, Zeyu Cui, Zhenru Zhang, Zihan Qiu, et al. 2025. Qwen2.5 Technical Report. *arXiv:2412.15115* [cs.CL] <https://arxiv.org/abs/2412.15115>
- [27] Nina Rimsky, Nick Gabrieli, Julian Schulz, Meg Tong, Evan Hubinger, and Alexander Turner. 2024. Steering llama 2 via contrastive activation addition. In *Proceedings of the 62nd Annual Meeting of the Association for Computational Linguistics (Volume 1: Long Papers)*. 15504–15522.
- [28] Devendra Sachan, Mike Lewis, Mandar Joshi, Armen Aghajanyan, Wen-tau Yih, Joelle Pineau, and Luke Zettlemoyer. 2022. Improving passage retrieval with zero-shot question generation. In *Proceedings of the 2022 Conference on Empirical Methods in Natural Language Processing*. 3781–3797.
- [29] Murray Shanahan, Kyle McDonell, and Laria Reynolds. 2023. Role play with large language models. *Nature* 623, 7987 (2023), 493–498.
- [30] Shuoqi Sun, Shengyao Zhuang, Shuai Wang, and Guido Zuccon. 2025. An investigation of prompt variations for zero-shot ILM-based rankers. In *European Conference on Information Retrieval*. Springer, 185–201.
- [31] Weiwei Sun, Lingyong Yan, Xinyu Ma, Shuaiqiang Wang, Pengjie Ren, Zhumin Chen, Dawei Yin, and Zhaochun Ren. 2023. Is ChatGPT good at search? investigating large language models as re-ranking agents. *arXiv preprint arXiv:2304.09542* (2023).
- [32] Nandan Thakur, Nils Reimers, Andreas Rücklé, Abhishek Srivastava, and Iryna Gurevych. 2021. Beir: A heterogenous benchmark for zero-shot evaluation of information retrieval models. *arXiv preprint arXiv:2104.08663* (2021).
- [33] Alexander Matt Turner, Lisa Thiergart, Gavin Leech, David Udell, Juan J Vazquez, Ulisse Mini, and Monte MacDiarmid. 2023. Steering language models with activation engineering. *arXiv preprint arXiv:2308.10248* (2023).
- [34] Anyi Wang, Dong Shu, Yifan Wang, Yunpu Ma, and Mengnan Du. 2025. Improving LLM Reasoning through Interpretable Role-Playing Steering. *arXiv preprint arXiv:2506.07335* (2025).
- [35] Noah Wang, Zy Peng, Haoran Que, Jiaheng Liu, Wangchunshu Zhou, Yuhan Wu, Hongcheng Guo, Ruitong Gan, Zehao Ni, Jian Yang, et al. 2024. Roleilm: Benchmarking, eliciting, and enhancing role-playing abilities of large language models. In *Findings of the Association for Computational Linguistics: ACL 2024*. 14743–14777.
- [36] Tianlong Wang, Xianfeng Jiao, Yinghao Zhu, Zhongzhi Chen, Yifan He, Xu Chu, Junyi Gao, Yasha Wang, and Liantao Ma. 2025. Adaptive Activation Steering: A Tuning-Free LLM Truthfulness Improvement Method for Diverse Hallucinations Categories. In *Proceedings of the ACM on Web Conference 2025 (Sydney NSW, Australia) (WWW '25)*. Association for Computing Machinery, New York, NY, USA, 2562–2578. doi:10.1145/3696410.3714640

[37] Yumeng Wang, Jirui Qi, Catherine Chen, Panagiotis Eustratiadis, and Suzan Verberne. 2025. How role-play shapes relevance judgment in zero-shot LLM rankers. *arXiv preprint arXiv:2510.17535* (2025).

[38] Jason Wei, Xuezhi Wang, Dale Schuurmans, Maarten Bosma, Fei Xia, Ed Chi, Quoc V Le, Denny Zhou, et al. 2022. Chain-of-thought prompting elicits reasoning in large language models. *Advances in neural information processing systems* 35 (2022), 24824–24837.

[39] Fred Zhang and Neel Nanda. 2023. Towards best practices of activation patching in language models: Metrics and methods. *arXiv preprint arXiv:2309.16042* (2023).

[40] Weixiang Zhao, Jiahe Guo, Yulin Hu, Yang Deng, An Zhang, Xingyu Sui, Xinyang Han, Yanyan Zhao, Bing Qin, Tat-Seng Chua, and Ting Liu. 2025. AdaSteer: Your Aligned LLM is Inherently an Adaptive Jailbreak Defender. In *Proceedings of the 2025 Conference on Empirical Methods in Natural Language Processing*, Christos Christodoulopoulos, Tammooy Chakraborty, Carolyn Rose, and Violet Peng (Eds.). Association for Computational Linguistics, Suzhou, China, 24559–24577. [doi:10.18653/v1/2025.emnlp-main.1248](https://doi.org/10.18653/v1/2025.emnlp-main.1248)

[41] Honglei Zhuang, Zhen Qin, Kai Hui, Junru Wu, Le Yan, Xuanhui Wang, and Michael Bendersky. 2024. Beyond yes and no: Improving zero-shot llm rankers via scoring fine-grained relevance labels. In *Proceedings of the 2024 conference of the North American chapter of the Association for Computational Linguistics: Human language technologies (volume 2: short papers)*. 358–370.

[42] Honglei Zhuang, Zhen Qin, Rolf Jagerman, Kai Hui, Ji Ma, Jing Lu, Jianmo Ni, Xuanhui Wang, and Michael Bendersky. 2023. Rankt5: Fine-tuning t5 for text ranking with ranking losses. In *Proceedings of the 46th International ACM SIGIR Conference on Research and Development in Information Retrieval*. 2308–2313.

[43] Shengyao Zhuang, Bing Liu, Bevan Koopman, and Guido Zuccon. 2023. Open-source large language models are strong zero-shot query likelihood models for document ranking. *arXiv preprint arXiv:2310.13243* (2023).

[44] Shengyao Zhuang, Honglei Zhuang, Bevan Koopman, and Guido Zuccon. 2024. A setwise approach for effective and highly efficient zero-shot ranking with large language models. In *Proceedings of the 47th International ACM SIGIR Conference on Research and Development in Information Retrieval*. 38–47.

[45] Andy Zou, Long Pham, Sarah Chen, James Campbell, Phillip Guo, Richard Ren, Alexander Pan, Xuwang Yin, Mantas Mazeika, Ann-Kathrin Dombrowski, et al. 2023. Representation engineering: A top-down approach to ai transparency. *arXiv preprint arXiv:2310.01405* (2023).